DALTON
FULL PAPER

Crystal architecture and magnetic properties of four transition-metal adipate coordination polymers

Evangelos G. Bakalbassis,*[a] Maria Korabik,[b] Adonis Michailides*[c] Jerzy Mrozinski,[b] Catherine Raptopoulou,[d] Stavroula Skoulika,[c] Aris Terzis*[d] and Dimitris Tsaousis[c]

[a] *Department of General and Inorganic Chemistry, Faculty of Chemistry, Aristotle University of Thessaloniki, Thessaloniki, Greece*
[b] *Faculty of Chemistry, University of Wroclaw, Wroclaw, Poland*
[c] *Department of Physical Chemistry, Faculty of Chemistry, University of Ioannina, Ioannina, Greece*
[d] *Institute of Material Science, NCSR Demokritos, Athens, Greece*

Received 13th November 2000, Accepted 31st January 2001
First published as an Advance Article on the web 28th February 2001

The crystal structures have been determined and the magnetic properties investigated for four novel $[M^{II}(A)(H_2O)_m]_n$ polymeric complexes, where M^{II} = Cd^{II}, Cu^{II} or Ni^{II}, m = 2–4 and A = adipate dianion. In $[Cd(A)(H_2O)_2]_n$ **1**, $[Cu(A)(H_2O)_2]_n$ **2** and $[Ni(A)(H_2O)_4]_n$ **4** the combination of the metal cation with the dicarboxylate ligand leads to the formation of infinitive chains; still the co-ordinated water molecules and the carboxylate oxygen atoms collaborate to hydrogen-bond the chains into 3-D structures. Each cadmium(II) and nickel(II) ion in **1** and **4** is coordinated in an octahedral geometry to carboxylate and water molecules. The coordination sphere around copper(II) ions in **2** is square planar. The structure of **3**, $[Cu_3(A)_2(OH)_2(H_2O)_4]_n$, is made up of ribbons linked to neighboring ones by hydrogen bonds. Each ribbon is composed of 2 crystallographically independent metal centers, Cu(1) and Cu(2), which exhibit octahedral and square pyramidal coordination geometries, respectively. Weak antiferromagnetic interactions were observed for **2**, and **3** (singlet–triplet energy gap values of -2.3 and -54.5 cm^{-1}, respectively) and isolated nickel(II) ions for **4**. An interpretation of the magnetic behavior was attempted. The strategy for the assembly of 1-D metal–organic chains into 3-D structures, with the use of coordinated water molecules as hydrogen bond donors and carboxylate oxygens as hydrogen bond acceptors, is also discussed.

Introduction

The controlled assembly of structural units in the solid state is essential for the rational synthesis of functional materials. Modern theoretical chemistry[1] provides reliable tools for the design of new molecules but the design of the packing in the solid state is still a difficult task[2] and empirical tools must be devised in order to achieve the synthesis of the desired material. These tools essentially consist of using appropriate directional links between the structural units, mainly hydrogen bonds (supramolecular assemblies)[3] and coordination bonds (coordination polymers).[4] An alternative method is to combine metal–ligand coordination with hydrogen bonding, by utilizing the hydrogen bonding capability of coordinated ligands.[5] This last method might be particularly interesting for the assembly of 3-D solids, especially in cases where a cooperative effect (magnetic, optical, *etc*.) is to be transmitted in the three directions of the space.

In the present study we investigate the synthesis, crystal structure and magnetic properties of some coordination polymers based on metal(II) centers (Cd^{II}, Cu^{II} and Ni^{II}), adipate anions (A) and water molecules. Moreover, a possible interpretation of the magnetic behavior, in correlation with the structural data and the results of quantum-chemical calculations, is attempted. Kubo and co-workers[6] have measured the magnetic susceptibility at room temperature of copper(II) salts of some α,ω-dicarboxylic acids including adipic acid. Despite the lack of single-crystal structure data in their study, our powdered-products synthetic strategy was that used in this paper. Moreover, the structure of nickel(II) adipate had been determined previously by Gupta and Saha[7] but complete structural information was not given. As in the case of cadmium(II) terephthalate,[8] it was expected that infinite coordination chains of the type –A–M^{II}–A– would result, held together by hydrogen bonds formed by the carboxylate oxygen atoms and the coordinated water molecules. Since no aromatic π–π interactions are present to induce stacking of the chains it was expected that the orientation and the spacing of the chains in the crystal would essentially depend on the geometry of the hydrogen bonding. Of specific interest would be the possibility of realizing 1-D or 2-D arrays of metal cations *via* hydrogen bonding.[9] In this context, the use of three different metal centers would permit a study of the influence of the coordination sphere on the supramolecular organization of these materials. Furthermore, in the case of the paramagnetic metal ions (Cu^{II} and Ni^{II}) it would also be expected that the bridging hydrogen bonds could provide pathways for magnetic exchange interactions.[10]

Experimental

Syntheses

Complex 1, $[Cd(A)(H_2O)_2]_n$. Colorless transparent single crystals were formed, within a few days at room temperature, by slow evaporation of an aqueous solution resulting from the mixing of equal volumes (10 cm^3) of $Cd(NO_3)_2$ (1.0 mmol) and adipic acid (1.0 mmol) at pH 6.

Complex 2, $[Cu(A)(H_2O)_2]_n$. (a) Single crystals of this compound were prepared by the silica gel method as follows: a sodium silicate solution (3 cm^3, Merck, d = 1.06 g cm^{-3}) was slowly added, under vigorous stirring, to an aqueous solution mixture of 1 M HNO_3 (0.5 cm^3) and adipic acid (10 cm^3, 1 mmol). The final pH after addition of the silica was about 6.

 DOI: 10.1039/b009075l

The gelling solution was poured into a test tube and allowed to stand for 24 h. Then, an aqueous solution of $Cu(NO_3)_2$ (10 cm^3, 1 mmol) was added at the top of the gel. Very thin green needles were formed near the liquid–gel interface within a few hours. After about four months the green needles began to transform into deep blue trapezoidal platelets. The conversion was quantitative after two months. Examination of the growth tubes under an optical stereoscope showed that, sometimes, a few blue-green platelets were also formed which were later found to be complex **3** (see below).

(b) Complex **2**, in powder form, was prepared by mixing, with continuous magnetic stirring, aqueous, equimolar (20 mmol) solutions of equal volumes (40 cm^3) of $Cu(NO_3)_2$ and adipic acid, at pH 6. A green solid precipitated almost immediately and transformed quantitatively into a deep blue solid after about 20 min. The blue precipitate was abundantly washed with cold water and dried in air. The X-ray powder diffraction (XRPD) pattern of this material was in good agreement with the simulated pattern reproduced from the F_c values of the calculated crystal structure. Thermal analysis showed that this compound decomposes at 260 °C.

Complex 3, $[Cu_3(A)_2(OH)_2(H_2O)_4]_n$. (a) Blue-green single crystals were prepared as described above. (b) Complex **3**, in powder form, was prepared by mixing, with continuous magnetic stirring, aqueous solutions of adipic acid (40 cm^3, 20 mmol) and copper acetate (135 cm^3, 27 mmol), at pH 6. The blue-green precipitate was abundantly washed with warm water (60 °C). The experimental XRPD pattern was in good agreement with the simulated one. This compound decomposes at almost 240 °C.

Complex 4, $[Ni(A)(H_2O)_4]_n$. (a) Single crystals of complex **4** were prepared as follows: a sodium silicate solution (2.5 cm^3, Merck $d = 1.06$ g cm^{-3}) was slowly added, under vigorous stirring, to an aqueous solution mixture of 1 M HNO_3 (0.5 cm^3) and adipic acid (10 cm^3, 3.33 mmol). The gelling solution was poured into a test tube and allowed to stand for about 24 h. An aqueous solution of $Ni(NO_3)_2$ (10 cm^3, 3.33 mmol) was added at the top of the gel. Many small transparent green platelets were formed near the interface within a few days. Then the supernatant liquid was removed and ethanol (10 cm^3) added at the top of the gel. The diffusion process was accelerated by partly destroying the interface with a glass rod. Single crystals were obtained within a few days.

(b) Complex **4**, in powder form, was prepared by mixing equal volumes (40 cm^3) of aqueous solutions of adipic acid (20 mmol) and $Ni(NO_3)_2$ (500 mmol). No precipitate was formed under these conditions. The mixture was stirred magnetically for about 10 min and left to evaporate for 20 days. The green precipitate formed was washed with water and dried in air. The simulated and experimental XRPD patterns were in good agreement. (Found: C, 24.58; H, 4.13. Calc. for $C_6H_{12}CdO_6$ **1**: C, 24.61; H, 4.11. Found: C, 29.25; H, 4.95. Calc. for $C_6H_{12}CuO_6$ **2**: C, 29.55; H, 4.90. Found: C, 24.94; H, 4.88. Calc. for $C_{12}H_{26}Cu_3O_{14}$ **3**: C, 24.64; H, 4.45. Found: C, 26.05; H, 5.77. Calc. for $C_6H_{16}NiO_8$ **4**: C, 26.19; H, 5.82%). IR (KBr disc): $\tilde{\nu}/cm^{-1}$ 3450 (**1**), 3220 (**1**), 1540 (**1**), 1405 (**1**), 3195 (**2**), 1565 (**2**), 1383 (**2**), 3320 (**3**), 3170 (**3**), 1525 (**3**), 1390 (**3**), 3480 (**4**), 3172 (**4**), 1516 (**4**) and 1397 (**4**).

Physical measurements

The IR spectra were recorded on a Perkin-Elmer 577 spectrophotometer using the KBr pellet technique. X-Ray powder diffraction spectra were recorded on a Siemens D500 diffractometer. Simulation of the spectra was carried out with the CaRIne Crystallography 3.1 software.[11] Magnetic susceptibility measurements at 1.75–300 K were carried out on powdered samples of the complexes, at a magnetic field of 5 kG, using a Quantum Design SQUID Magnetometer (type MPMS-5). Susceptibility data were corrected for the diamagnetism of the constituent atoms using Pascal's constants.[12] The temperature-independent paramagnetism (TIP) values used for Cu^{II} and Ni^{II} were 60×10^{-6} and 229×10^{-6} cm^3 mol^{-1}, respectively. The effective magnetic moment for Cu^{II} was calculated from the equation $\mu_{eff} = 2.83(\chi_m T)^{1/2}$ μ_B. The EPR spectra were recorded at X-band on an ESP 300 Bruker spectrometer, at room temperature, 77 and 4.2 K, equipped with an ER 035M Bruker NMR gaussmeter and a HP 5350B Hewlett-Packard microwave frequency counter.

Crystallography

Crystal data. *Complex* ***1***. $C_6H_{12}CdO_6$, $M = 292.41$, monoclinic, space group $C2/c$, $a = 16.523(7)$, $b = 5.585(2)$, $c = 11.089(5)$ Å, $\beta = 95.53(1)°$, $U = 1018.7(8)$ $Å^3$, $Z = 4$, $\mu = 21.41$ cm^{-1}, 1105 unique (N) reflections ($R_{int} = 0.0109$), of which 1042 ($I > 2.0\sigma(I)$) were used (N_o) in all calculations. Final $R1 = 0.0220$ and $wR2 = 0.0561$.

Complex ***2***. $C_6H_{12}CuO_6$, $M = 243.70$, triclinic, space group $P\bar{1}$, $a = 4.929(2)$, $b = 11.328(4)$, $c = 3.866(1)$ Å, $\alpha = 87.09(1)$, $\beta = 83.47(1)$, $\gamma = 84.31(1)°$, $U = 213.2(1)$ $Å^3$, $Z = 1$, $\mu = 25.57$ cm^{-1}, $N = 744$ ($R_{int} = 0.0104$), $N_o = 741$ ($I > 2.0\sigma(I)$), $R1 = 0.0200$, $wR2 = 0.0535$.

Complex ***3***. $C_{12}H_{26}Cu_3O_{14}$, $M = 586.96$, triclinic, space group $P\bar{1}$, $a = 5.727(3)$, $b = 7.455(4)$, $c = 12.648(6)$ Å, $\alpha = 97.70(1)$, $\beta = 104.16(1)$, $\gamma = 106.44(1)°$, $U = 490.1(4)$ $Å^3$, $Z = 2$, $\mu = 32.96$ cm^{-1}, $N = 1722$ ($R_{int} = 0.0146$), $N_o = 1442$ ($I > 2.0\sigma(I)$), $R1 = 0.0381$, $wR2 = 0.0937$.

Complex ***4***. $C_6H_{16}NiO_8$, $M = 247.90$, monoclinic, space group $P2_1/c$, $a = 4.781(1)$, $b = 9.780(2)$, $c = 11.648(3)$ Å, $\beta = 98.927(8)°$, $U = 538.1(2)$ $Å^3$, $Z = 2$, $\mu = 28.78$ cm^{-1}, $N = 911$ ($R_{int} = 0.0290$), $N_o = 827$ ($I > 2.0\sigma(I)$), $R1 = 0.0476$, $wR2 = 0.1271$.

For all complexes data were collected at 298 K. The structures were solved with SHELXS 86[13] and refined using SHELXL 93.[14]

CCDC reference numbers 152778–152781.

See http://www.rsc.org/suppdata/dt/b0/b009075l/ for crystallographic data in CIF or other electronic format.

Results and discussion

EPR spectra

The EPR spectrum for a solid sample of **2**, showed only two features, with $g_\parallel > g_\perp$ at room temperature, 77 and/or 4.2 K, accounting well for a $|x^2 - y^2>$ ground state. The spectroscopic splitting parameters obtained at all previous temperatures were identical ($g_\parallel = 2.340$, $g_\perp = 2.051$, $g_{av} = 2.155$). **3** remained EPR silent, upon cooling from room temperature to 77 K; however, at 4.2 K it showed an isotropic signal, at 3150 G, with $g = 2.102$.

Crystal structures

The crystal structure of complex **1** is shown in Fig. 1. The cadmium ion is located on a twofold symmetry axis and is coordinated in a distorted octahedral geometry by six oxygen atoms, two of which belong to two symmetry related water molecules, the four remaining being carboxylate oxygen atoms. Selected bond lengths and angles are shown in Table 1. The adipate(2−) ligand acts in the bis-bidentate chelating mode which is predominant in all cadmium carboxylates.[15] As a result infinite zigzag chains are formed (Fig. 2). Similar chains have also been observed recently in the structure of cadmium terephthalate,[8] but in the present case the packing is quite different. The chains are connected through relatively strong hydrogen bonds along both b (Fig. 1) and c (Fig. 2) directions, but the corresponding synthons[16] are not the same. In particular, along the b axis two donor atoms bonded to the same metal interact with two complementary acceptor atoms attached to a neighboring metal center. The Cd · · · Cd distance in this direc-

Table 1 Selected bond distances (Å) and angles (°) for complex **1**

Cd–O(1w)	2.229(2)	Cd–O(1)	2.323(2)	Cd–O(2)	2.350(2)
O(1w)–Cd–O(1w)[a]	96.92(13)	O(1)–Cd–O(1)[a]	159.16(14)	O(1w)–Cd–O(2)	146.17(8)
O(1w)–Cd–O(1)	91.36(8)	O(1w)–Cd–O(2)[a]	97.48(9)	O(1)–Cd–O(2)	55.64(7)
O(1w)[a]–Cd–O(1)	102.48(10)	O(1)–Cd–O(2)[a]	107.60(9)	O(2)[a]–Cd–O(2)	87.15(11)
Hydrogen bonding					
O(1w)–O(1)[b]	2.692(3)	O(1w)[c]–O(2)	2.742(3)		
O(1w)[c]–H(Bw)[c]–O(2)	173.4	O(1w)–H(Aw)–O(1)[b]	169.9		

Symmetry transformations used to generate equivalent atoms: (*a*) $-x, y, 0.5 - z$; (*b*) $-x, -y, 1 - z$; (*c*) $-x, 1 + y, 0.5 - z$.

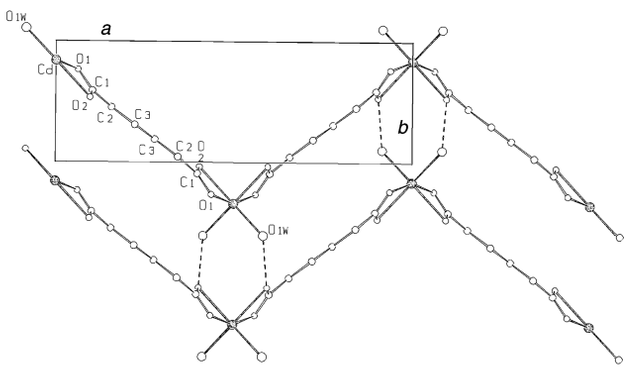

Fig. 1 The zigzag chains of complex **1**, connected through hydrogen bonds along the *b* axis, together with the coordination sphere of Cd^{II}. Interchain hydrogen bonds are shown as dashed lines.

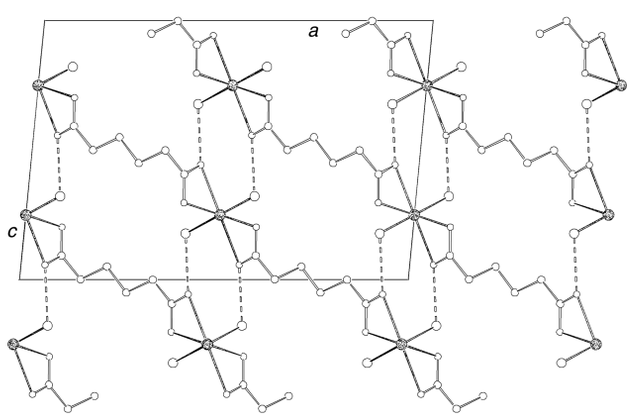

Fig. 2 The hydrogen bonding interactions connecting the neighboring chains in complex **1**.

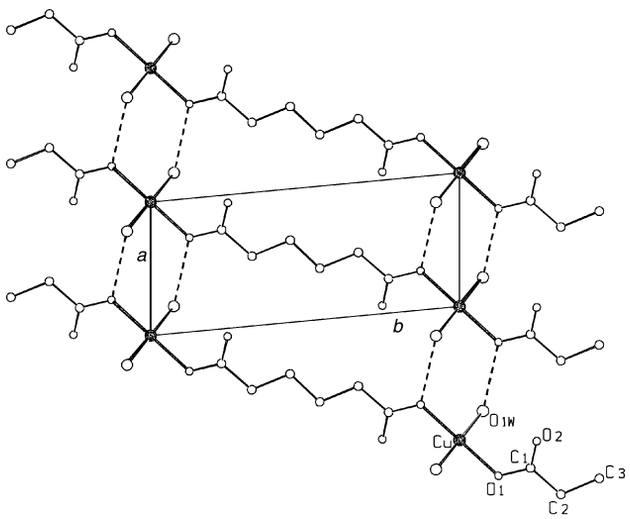

Fig. 3 The hydrogen bonded chains of complex **2** along the *a* axis, together with the coordination sphere of Cu^{II}.

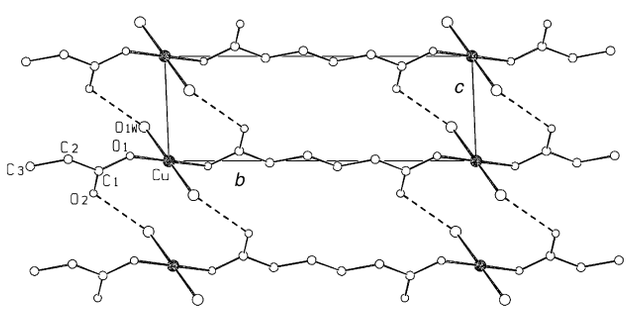

Fig. 4 The hydrogen bonded chains of complex **2** along the *c* axis.

tion is the repeat of the *b* axis (5.585 Å). The first order graph-set[17] (hereafter denoted as N1) describing this synthon is $R_2^2(8)$. In the *c* direction the hydrogen bonding is described by the same graph-set notation, but, in this case, the metal center provides a pair of donor/acceptor atoms. The metal spacing is half of the *c* axis (5.544 Å).

The structure of complex **2** is illustrated in Fig. 3. The metal occupies a crystallographic inversion center; its coordination geometry, involving two carboxylate oxygen atoms and two water molecules, is strictly square planar. Both Cu–O(1) and Cu–O(1w) bond distances are (see Table 2) in the normal range observed for analogous copper(II) acetato-bridged complexes.[18] The adipate dianions act in the bis-unidentate coordination mode and bridge the copper cations along the direction of the diagonal of the *ab* plane.The infinite chains thus formed are held together *via* strong hydrogen bonds (Table 2), leading to a 3-D architecture. Along the *c* and *a* axes directions the hydrogen links involve two aqua ligands (donors) and two carboxylate oxygen atoms (acceptors), but the corresponding supramolecular synthons are different. It is clear from Fig. 3 that in the direction of the *a* axis the synthons comprise only the coordinated carboxylate oxygens; the thus formed sheets are parallel to the *ab* plane. These synthons are described by N1 = $R_2^2(8)$ while the second order graph-set notation (hereafter denoted as N2) is $C_4[R_2^2(8)]$. The Cu · · · Cu distance is equal to the *a* axis length (4.929 Å). The synthons along the *c* axis direction involve the non-coordinated carboxylate oxygens (Fig. 4) and the resulting sheets are parallel to the *bc* plane. These synthons are described by N1 = $R_2^2(12)$ and N2 = $C_6[R_2^2(12)]$. In this case, the Cu · · · Cu distance along *c* equals the length of the axis (3.866 Å), too.

The structure of complex **3** is made up of ribbons of $[Cu_3(C_6H_8O_4)_2(OH)_2(H_2O)_4]$ running parallel to the *a* axis (Fig. 5). The ribbon is composed of 2 crystallographically independent metal centers, Cu(1) and Cu(2), which exhibit elongated octahedral and square pyramidal coordination spheres, of the type CuO_6 and CuO_5, respectively. Cu(1) is located at a symmetry inversion center and its geometry is defined by two carboxylate oxygens (O(1) and its symmetry related one) belonging to two different adipate ligands using only one carboxylate group in coordination, two hydroxo anions (O(5) and its symmetry related one) and two water

Table 2 Selected bond distances (Å) and angles (°) for complex **2**

Cu–O(1w)	1.968(2)	Cu–O(1)	1.9305(14)	Cu–O(2)	3.016(3)
O(1)–Cu–O(1) [a]	180.0	O(1) [a]–Cu–O(1w)	180.0	O(1)–Cu–O(1w)	90.81(7)
Hydrogen bonding					
O(1w)–O(1) [b]	2.692(2)	O(1w)–O(2) [c]	2.632(2)		
O(1w)–H(Aw)–O(1) [b]	175.3	O(1w)–H(Bw)–O(2) [c]	166.7		

Symmetry transformations used to generate equivalent atoms: (*a*) $-x, -y, -z$; (*b*) $1 + x, y, z$; (*c*) $x, y, 1 + z$.

Table 3 Selected bond distances (Å) and angles (°) for complex **3**

Cu(1)–O(1)	1.933(3)	Cu(1)–O(5)	2.016(3)	Cu(1)–O(2w)	2.335(4)
Cu(2)–O(5) [a]	1.977(3)	Cu(2)–O(1w)	1.948(4)	Cu(2)–O(2)	1.946(3)
Cu(2)–O(5)	1.974(3)	Cu(2)–O(2w) [a]	2.404(4)		
O(1) [b]–Cu(1)–O(1)	180.0	O(1)–Cu(1)–O(5) [b]	86.659(3)	O(1)–Cu(1)–O(5)	93.35(13)
O(5) [b]–Cu(1)–O(2w)	95.63(13)	O(5) [b]–Cu(1)–O(5)	180.0	O(1) [b]–Cu(1)–O(2w)	93.35(13)
O(1)–Cu–O(2w)	93.62(14)	O(5)–Cu(1)–O(2w)	84.37(13)	O(2w)–Cu(1)–O(2w) [b]	180.0
O(2)–Cu(2)–O(1w)	87.63(16)	O(2)–Cu(2)–O(5)	171.71(14)	O(1w)–Cu(2)–O(5)	97.31(15)
O(2)–Cu(2)–O(5) [a]	93.66(14)	O(1w)–Cu(2)–O(5) [a]	176.31(14)	O(5)–Cu(2)–O(5) [a]	81.83(13)
O(2)–Cu(2)–O(2w) [a]	96.52(15)	O(1w)–Cu(2)–O(2w) [a]	93.02(15)	O(5)–Cu(2)–O(2w) [a]	89.89(13)
O(5)–Cu(2)–O(2w) [a]	83.40(13)				
Hydrogen bonding					
O(1w)–O(3) [c]	2.714(6)	O(1w)–O(4) [d]	2.659(5)	O(2w)–O(3) [e]	2.798(5)
O(2w)–O(4) [f]	2.779(5)				
		O(1w)–H(1Bw)–O(3) [c]	158.1	O(1w)–H(1Aw)–O(4) [d]	153.1
O(2w)–H(2Bw)–O(3) [e]	165.7	O(2w)–H(2Aw)–O(4) [f]	162.4		

Symmetry transformations used to generate equivalent atoms: (*a*) $1 - x, 1 - y, 1 - z$; (*b*) $-x, 1 - y, 1 - z$; (*c*) $x, y - 1, z - 1$; (*d*) $x - 1, y - 1, z - 1$; (*e*) $x, y, z - 1$; (*f*) $1 - x, 2 - y, 2 - z$.

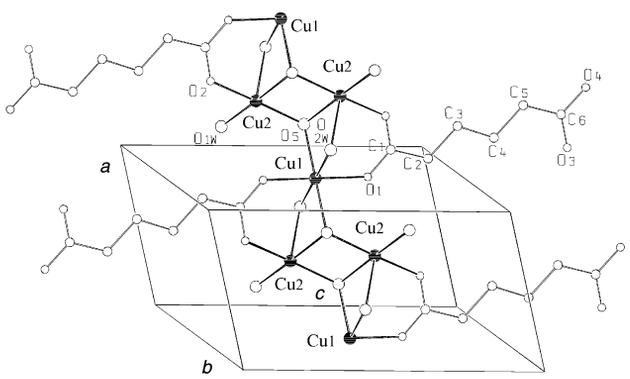

Fig. 5 A view of the ribbon in complex **3**, showing the coordination spheres of Cu(2) and Cu(1).

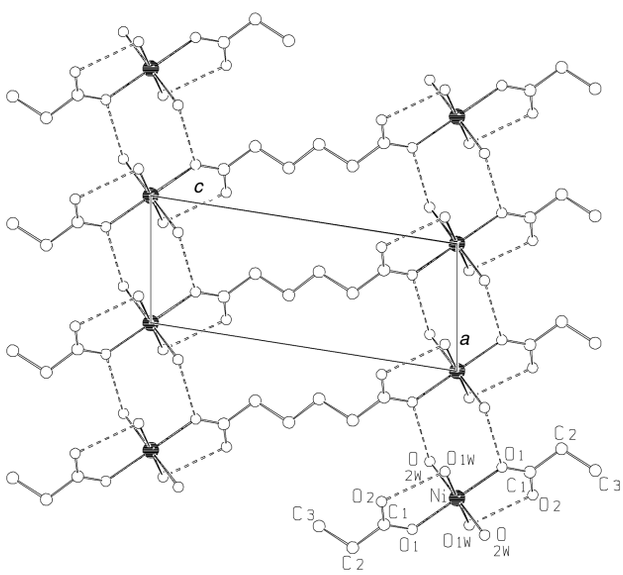

Fig. 6 The hydrogen bonded chains in complex **4** forming sheets parallel to the *ac* plane, together with the coordination sphere of Ni^{II}.

molecules (O(2w) and its symmetry related one). The water molecules occupy the axial positions; still, the second carboxylate anion of each adipate ligand remains pendant. All Cu–O bond lengths are (Table 3) in the normal range observed for analogous copper(II) complexes. The Cu(1) atom is bridged to a neighboring Cu(2) atom *via* a μ-water molecule (O(2w)), a μ_3-hydroxo ion (O(5)), and a μ-carboxylato-OCO group. The hydroxo ion further bridges both Cu(1) and Cu(2) to another Cu(2) atom. The Cu(2)–Cu(2) "dimers" are built around crystallographic inversion centers. The coordination sphere of Cu(2) is defined by two hydroxo ions, two water molecules and one carboxylate oxygen. The five donor atoms within bonding distances define a regular polyhedron around each Cu(2) atom. Analysis of the shape-determining angles, by using the approach of Reedijk *et al.*[19] yields a τ value of 0.08, hence the geometry around Cu(2) is almost perfect pyramidal. Two square pyramids of this type are joined together, by sharing one basal coordination site, to afford the Cu(2)–O(5)–Cu(2)–O(5) dimeric moiety. These moieties are planar; still the metal–metal distances in the Cu(2)–Cu(2) and Cu(1)–Cu(2) "dimers" are 3.397 and 3.053 Å, respectively, while the Cu(1)–Cu(2) inter-"dimer" distance is 3.397 Å. Each ribbon is linked to four neighboring ones by hydrogen bonds involving the aqua ligands O(1w) and O(2w), the hydroxyl ions O(5) and the non-coordinated carboxylate oxygen atoms.

Each nickel cation in the structure of complex **4** is located on a center of symmetry and is octahedrally coordinated by six oxygen atoms belonging to four water molecules and two different bis-unidentately coordinated adipate anions (Fig. 6). Owing to almost equal Ni–O bond distances and the O(1w)–Ni–O(1w), O(2w)–Ni–O(2w) and O(1)–Ni–O(1) angle values of 180° (Table 4), the coordination geometry around Ni^{II} is a regular octahedral one. All Ni–O coordination bond lengths are

Table 4 Selected bond distances (Å) and angles (°) for complex **4**

Ni–O(1)	2.061(2)	Ni–O(1w)	2.056(2)	Ni–O(2w)	2.067(2)
O(1w)[a]–Ni–O(1w)	180.0	O(1w)–Ni–O(1)[a]	89.10(9)	O(2w)–Ni–O(2w)[a]	180.0
O(1w)–Ni–O(2w)	88.33(9)	O(1)–Ni–O(2w)	88.66(9)	O(1)–Ni–O(1)[a]	180.0
Hydrogen bonding					
O(1w)–O(2)	2.636(3)	O(2w)–H(2Aw)–O(1)[b]	165.4		
O(2w)–O(1)[b]	2.686(3)	O(1w)–H(1Aw)–O(2)	158.7		
O(2w)–O(2)[c]	2.740(3)	O(2w)–H(2Bw)–O(2)[c]	166.4		

Symmetry transformations used to generate equivalent atoms: (*a*) $-x, 1-y, 1-z$; (*b*) $1-x, 1-y, 1-z$; (*c*) $x, 0.5-y, z-0.5$.

Table 5 Construction characteristics of polymers **1**, **2** and **4**

		1	**2**	**4**
Symmetry of the ligand		$\bar{1}$	$\bar{1}$	$\bar{1}$
Coordination geometry		Octahedral	Square planar	Octahedral
Symmetry of the metal center		2-fold axis	$\bar{1}$	$\bar{1}$
Layer group symmetry		*P*2/*c*	$P\bar{1}$	$P\bar{1}$
Space group symmetry		*C*2/*c*	$P\bar{1}$	$P2_1/c$
First-order graph set/metal–metal separation/Å	a	—	$R_2^2(8)$/4.93	$R_2^2(8)$/4.78
	b	$R_2^2(8)$/5.58	—	—
	c	$R_2^2(8)$/5.54	$R_2^2(12)$/3.87	—

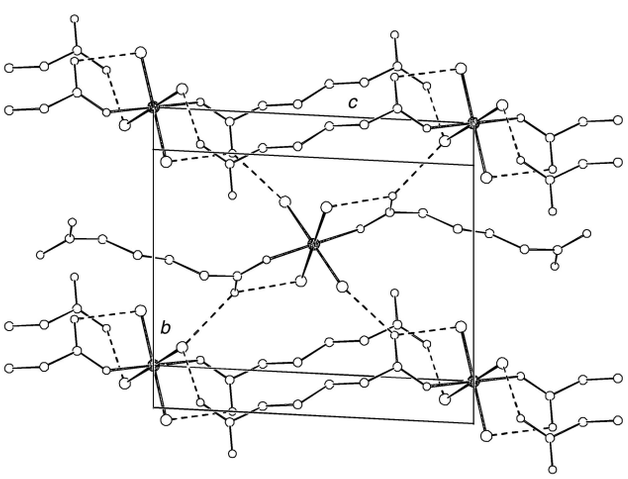

Fig. 7 The additional hydrogen bonds connecting the sheets together in complex **4**.

within the normal range observed for other structurally characterized nickel(II) hydroxo- and acetato-bridged complexes.[20] The thus formed chains are hydrogen-bonded to form sheets parallel to the *ac* plane. The hydrogen bonds are described by $N1 = R_2^2(8)$ leading to a 4.781 Å repeat along the *a* axis and $N2 = C_4[R_2^2(8)]$. The sheets are connected by additional hydrogen bonds involving the water molecules and the non-coordinated carboxylate oxygens (Fig. 7). The latter atoms participate also in "intra- molecular" hydrogen bonds.

Hydrogen bonding and supramolecular organization

The presence of hydrogen bond donors and acceptors in close proximity in the coordination sphere of each metal cation allows for the formation of ring-type (R) hydrogen links between two neighboring metal–organic chains. Furthermore, the absence of other functional groups on the carbon skeleton of the ligand, ensures that all directional intermolecular interactions (hydrogen bonds) will occur "around" the metal. This means that in the case of ring-type hydrogen bonds the symmetry operator generating this interaction will probably either lie on the center of the ring (inversion centers in compounds **2** and **4**), or pass through it (2-fold axis in **1**). The construction characteristics of these three polymeric compounds are summarised in Table 5. By use of this Table it is interesting to examine how the local symmetry operators combine to lead to layer group symmetry[21] and finally to the observed space group. We may remark that in compound **2** the interaction between successive layers is achieved by simple translation while in **1** and **4** an offset generated by a 2_1 axis is required.

Phase transformations of copper(II) adipates

The blue phase of copper adipate (see Experimental section) is always obtained from a green one that precipitates first. This blue phase remains indefinitely stable but it transforms (reversibly) into the green one if heated at 60 °C in its mother liquor. Also, if copper acetate instead of copper nitrate is used as the metal source two phases are obtained depending on whether the precipitate is washed with warm (compound **3**) or cold water (non-identified phase). Therefore, the copper adipate phase described by Kubo and co-workers,[6,22] is probably a mixture, since its IR spectrum shows significant differences from ours. The question that arises is why so many phases are present in the Cu^{II}/adipic acid system (pH 6)? The proximity of the metal centers in **2** lets us assume that the carboxylate group can rotate and bridge two neighboring metal cations to yield the green phase. This is supported by the IR spectrum (KBr pellet) of this phase, exhibiting a difference, Δ, between the asymmetric (1550 cm^{-1}) and the symmetric stretching vibration (1402 cm^{-1}), of 148 cm^{-1}, which may be attributed to the presence of bidentate bridging carboxylate groups.[23] This is further supported by the presence of such groups in the green-blue complex, **3**, for which a Δ value of 135 cm^{-1} is derived. Transition from one complexing mode to the other in neighboring metal centers has been described and the term "carboxylate shift" used to designate this motion.[24]

Magnetic properties

The room temperature $\chi_m T$ value (0.400 $cm^3\ mol^{-1}\ K$) of complex **2** (Fig. 8) is what is expected for a non-coupled copper(II) ion. $\chi_m T$ decreases gradually with decreasing temperature, to *ca.* 40 K, where upon it decreases more rapidly exhibiting a value of *ca.* 0.025 $cm^3\ mol^{-1}$ K at 1.7 K. Qualitatively, the interpretation of this curve is as follows. Deviations from Curie behavior, not inconsistent with weak intramolecular antiferromagnetic interactions, are observed for the high-temperature

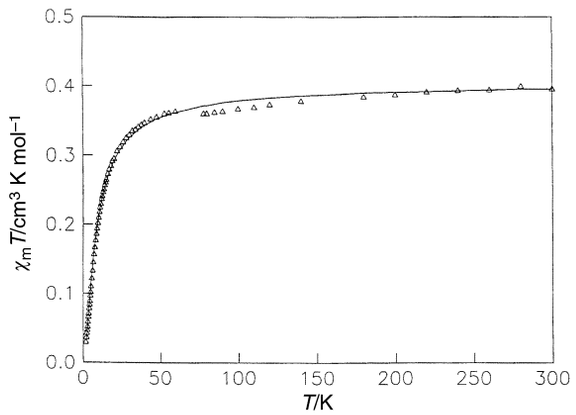

Fig. 8 Temperature dependence of $\chi_m T$ for complex **2**. The solid line is calculated with the parameters reported in the text.

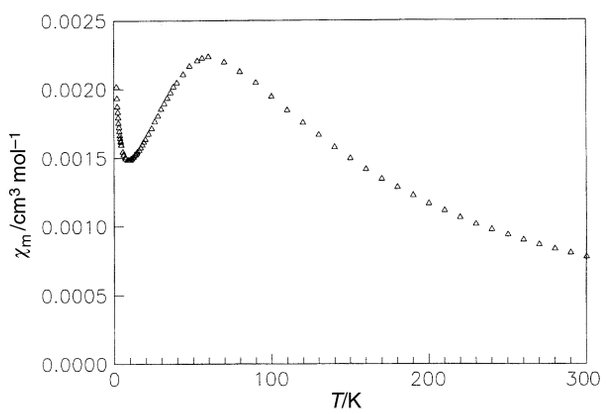

Fig. 9 Temperature dependence of χ_m for complex **3**.

range; still a very weak intermolecular antiferromagnetic interaction occurs below 40 K.

In an attempt to probe deeper into the magnetic superexchange interactions, the magnetic behavior of complex **2** is closely combined with its molecular and crystal structure. Hence, the susceptibility data were least-squares fitted by the high-temperature series expansion (1) for a 2-D square-planar

$$\chi_m = \frac{Ng^2\beta^2}{4kT}\left(1 + \frac{2}{x} + \frac{2}{x^2} + \frac{1.333}{x^3} + \frac{0.250}{x^4} - \frac{0.4833}{x^5} + \frac{0.003979}{x^6}\right)^{-1} + N_\alpha \quad (1)$$

antiferromagnet of Rushbrooke and co-workers,[25,26] where $x = kT/|J|$, with a molecular field correction to account for the interplane interactions. Least-squares fitting of the experimental susceptibility data in this equation gives $J = -2.3$ cm^{-1}, $zJ' = -0.13$ cm^{-1} and $g = 2.08$ ($R = 4.21 \times 10^{-2}$). This fit is shown in Fig. 8. The same discrepancy R value of $\sum_{i=1}^{n}[(\chi_m T)_{exp} - (\chi_m T)_{theor}]^2 / \sum_{i=1}^{n}[(\chi_m T)_{exp}]^2$ was used throughout the paper.

Variable-temperature (1.7–300 K) magnetic susceptibility data were collected for complex **3** and are shown in Fig. 9 in the form of the temperature dependence of the molar magnetic susceptibility, χ_m. The temperature dependence is very interesting, since it exhibits both a maximum at 78 K and a minimum at *ca.* 10 K. The crystal structure of **3** clearly shows that, along each zigzag chain, there is an alternation of two different fragments, *i.e.* that of a monomer and that of a dimer, connected through coordination bonds, hence they are not magnetically isolated. Consequently, from a magnetic point of view, it is difficult to construct a Hamiltonian along with a subsequent susceptibility equation, for calculation of the magnetic parameters for **3**. For this reason the Hamiltonian $\mathcal{H} = -2J\hat{S}_1\hat{S}_2 - zJ'\hat{S}_1\hat{S}_2$ was constructed, being a modified Heisenberg one including exchange interactions between monomeric and dimeric fragments of an infinite chain. The subsequent susceptibility equation is as in (2). Eqn. (2), has two

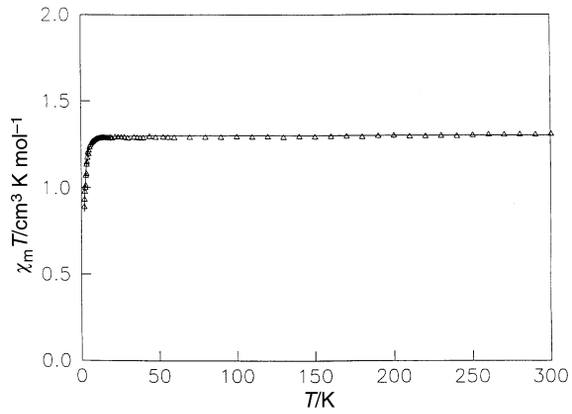

Fig. 10 Temperature dependence of $\chi_m T$ for complex **4**. The solid line is calculated with the parameters reported in the text.

$$\chi_m = \frac{2}{3}\left[\frac{Ng_A^2\beta^2}{k(T-\theta)}(3 + e^{-2J/kT})^{-1}\right] + \frac{1}{3}\left[\frac{Ng_B^2\beta^2}{4k(T-\theta)}\right] \quad (2)$$

main fragments concerning a pseudodimeric, A, and a pseudomonomeric, B, one. The two subsequent fragments are not magnetically isolated from the other magnetic centers. Moreover, since the Weiss constant concerns both parts of eqn. (1), fragments A and B are not additive. The magnetic interactions between neighboring magnetic centers play an important role on the magnetism of **3**.

Least-squares fitting of the susceptibility data, in the 80–300 K temperature region, where the $\chi_m^{-1} = f(T)$ function is linear, in eqn. (2) gives $J = -54.5$ cm^{-1}, $\theta = +2.8$ cm^{-1}, $g_A = 2.26$ and $g_B = 2.10$ (from EPR spectroscopy), $R = 2.41 \times 10^{-3}$.

Since the $\chi_m T$ value of complex **3** decreases gradually upon cooling from room temperature (0.408 cm^3 mol^{-1} K) to *ca.* 80 K (0.270 cm^3 mol^{-1} K), antiferromagnetic interactions should be expected for this complex, in close agreement with the results of our fitting. Moreover, the increase of the χ_m value (see Fig. 9) in the 10–1.7 K temperature range could be the result of the weak magnetism of the intervening copper(II) octahedral monomers, B, in each chain, after the completion of the coupling between the copper(II) ions inside each dimeric fragment, A.

The variation with temperature of the $\chi_m T$ product for complex **4** is illustrated in Fig. 10. The room temperature $\chi_m T$ value (1.24 cm^3 mol^{-1} K) is what is expected for an $S = 1$ Ni^{II}. The $\chi_m T$ curve remains parallel to the T axis upon cooling from room temperature to *ca.* 10 K, whereupon it decreases more rapidly reaching a value of *ca.* 0.75 cm^3 mol^{-1} K at 1.7 K.

The magnetic data of complex 4 were analysed by using the spin Hamiltonian $\mathcal{H} = DS_z^2 - g\beta HS - zJ'S\langle S\rangle$ where D is the zero-field splitting parameter, z the number of nearest neighbors around a given magnetic centre and J' the exchange parameter between two nearest-neighbor magnetic centres. The susceptibility eqn. (3) holds for the zero-field splitting of an

$$\chi_m = \frac{2Ng^2\beta^2}{3kT}\left(\frac{2x^{-1} - 2x^{-1}e^{-x} + e^{-x}}{1 + 2e^{-x}}\right) \quad (3)$$

isolated nickel(II) ion,[27] where $x = D/kT$ and χ_m the molar magnetic susceptibility per Ni^{II}. The molecular-field corrected susceptibility χ_i' is given by eqn. (4) ($i = \parallel$ or $\perp$) where χ_i' are the crystal-field susceptibilities and z the number of nearest

neighbor magnetic centres. Least-squares fitting of the experimental susceptibility data in eqn. (4) gives $D = 3.28$ cm^{-1}, $g = 2.28$,

$$\chi_i' = \frac{\chi_m}{1 - \left(\frac{2zJ}{Ng_i^2\beta^2}\right)\chi_m} \quad (4)$$

$zJ' = -0.04$ cm^{-1}, $R = 6.37 \times 10^{-3}$. This fit is shown in Fig. 10. The very small exchange parameter derived [$zJ' = -0.04$ cm^{-1}] could account for isolated nickel(II) ions in the crystal lattice.

Interpretation of the exchange mechanism

The magnetic exchange interaction mechanism is now examined. In complex **2** each magnetic orbital is built from a $d_{x^2-y^2}$ copper orbital pointing towards its nearest neighbor atoms, the two O(1) and the two O(1w) (see Fig. 3 and Table 2). The neighboring magnetic orbitals along the *a* axis are linked by hydrogen bonds between O(1) and O(w1), the corresponding Cu···Cu distance being 4.93 Å. Moreover, along the *c* axis two nearest neighbor magnetic orbitals are parallel to each other and on different planes (see Fig. 4). Two sequential magnetic orbitals of this kind are bridged by two carboxylate groups, the corresponding Cu···Cu distance being 3.866 Å. Finally, two magnetic orbitals of **2** are also bridged, along the *b* axis, by an adipate molecule, the corresponding Cu···Cu distance being 11.3281 Å. It is well known that a bridging moiety is most effective in supporting antiferromagnetic exchange interaction between two transition-metal magnetic ions if the bridge has available molecular orbitals that can interact with the bonding combination of two metal d orbitals.[28] Therefore, CNDO/2 molecular orbital calculations for the adipate bridge were carried out by employing the molecular dimensions of this bridge in the structure of **2**. The only occupied orbital of the bridge which could offer an effective pathway for an antiferromagnetic interaction between two copper(II) $d_{x^2-y^2}$ orbitals is its HOMO (Scheme 1). However, it possesses an

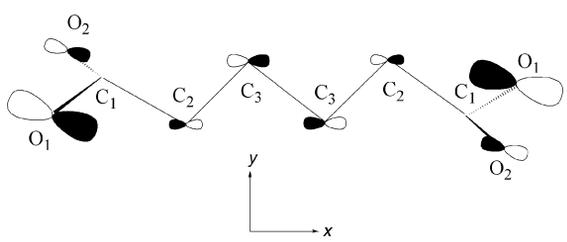

Scheme 1 The HOMO of the bridging adipate ligand.

incomplete effective p-type pathway between the $2p_x$ orbitals located at carbon atoms C(2) and C(3) only, since their $2p_x$ coefficients are very small and the C(1) one is zero. Hence, this orbital will not propagate any interaction due to the small and incomplete effective overlap at the chain C–C interactions.[29] Nevertheless, the capability of both hydrogen bonds[10] and carboxylate groups[30] to propagate the exchange interactions between two copper(II) magnetic centers has well been demonstrated. Consequently, the weak antiferromagnetic interaction, derived from the fitting procedure for **2**, could be possibly due to: (i) the weak interaction between the two magnetic orbitals of two nearest neighbor copper ions along the *c* axis (these orbitals are parallel to each other and on different planes[31]) and (ii) the weak interactions *via* hydrogen bonds[10] along the *a* axis. The interchain interaction seen in **2** could be attributed to its dense hydrogen-bonding network. Finally, based upon the orbital view of the HOMO, localized mainly at the σ-type hybrids of both O(1) atoms, the bis-unidentate coordination of the adipate bridging unit, found in **2**, can easily be explained.

Complex **3** has sets of three sequential magnetic orbitals along each zigzag chain. Two are the, much alike to each other, sequential Cu(2)- and Cu(2)-centered ones, involved in the Cu(2)O(5)Cu(2)O(5) dimeric moieties; the third is the Cu(1)-centered one. (see Fig. 5). In particular, each Cu(2)-centered magnetic orbital is built from a d_{xy} copper orbital pointing towards its nearest neighboring atoms, the two O(5), O(1w) and O(2). Consequently, there is no spin density on the O(2w) atom coming from the Cu(2) magnetic center. Moreover, each Cu(1)-centered magnetic orbital is built from a $d_{x^2-y^2}$ copper orbital pointing towards its nearest neighbor atoms, the two O(5) and two O(1). Again, there is no spin density on the O(2w) atom coming from the Cu(1) magnetic center. Apart from this latter O(2w) bridge, each Cu(2)···Cu(1) dimeric moiety also possesses two more bridges being, the hydroxo O(5) and the O(1)C(1)O(2) carboxylato moiety of an adipate ligand. However, the Cu(1)–Cu(2) exchange interaction, if any, should be very weak, since the corresponding Cu(1)- and Cu(2)-centered magnetic orbitals are almost orthogonal to each other (their dihedral angle value is of the order of *ca.* 83°).

It was shown above that the Cu(2)O(5)Cu(2)O(5) moieties are planar. Consequently, according to the magneto-structural correlations established by Hatfield and co-workers[32] for dihydroxo-bridged dicopper complexes, a J value of -74.19 cm^{-1} should correspond to a 98.54° Cu–O–Cu dihydroxo-bridged angle for the Cu(2)–Cu(2) exchange interaction. However, the triply bridging function of both μ-hydroxo bridges, O(5), could account well for the lower Cu(2)···Cu(2) interaction ($J = -54.5$ cm^{-1}) derived from the fitting procedure.

The two unpaired electrons of the nickel(II) ions in complex **4** occupy a $d_{x^2-y^2}$ and a d_{z^2} orbital pointing to both water and bridging carboxylate oxygen atoms. As a result, all the exchange couplings through the oxygen atoms should be consistent *a priori*, to be operative. Two sequential nickel(II) ions, along each chain of the complex (see Fig. 6), are bridged by an adipic acid dianion in a bis-unidentate fashion. Since the adipate bridging unit will not propagate any exchange interaction (see above), the magnetic isolation of the nickel(II) ions along each chain can be well understood. The interchain exchange interaction of **4** can be attributed to its dense hydrogen bonding network.

Conclusion

The crystal structures and the variable-temperature magnetic susceptibility measurements, described above, have shown that the use of coordinated water molecules as hydrogen bond donors and carboxylate oxygens as hydrogen bond acceptors is a successful strategy for (i) the formation of 1-D metal–organic chains, (ii) ring-type (R) hydrogen links between two neighboring metal–organic chains, and (iii) the assembly of 1-D metal–organic chains into 3-D structures; still the formation of arrays of paramagnetic metal centers *via* these bridges induced magnetic interactions, for both complexes **2** and **3**. Moreover, the absence of other functional groups on the carbon skeleton of the ligand ensured that all directional intermolecular interactions (hydrogen bonds) will occur "around" the metal. This means that, in the case of ring-type hydrogen bonds, the symmetry operator generating this interaction will probably either lie on the center of the ring (inversion centers in compounds **2** and **4**), or pass through it (2-fold axis in **1**). These observations may be useful for the design of solids with specific symmetry.

Acknowledgements

This work was financially supported in part by the State Committee for Scientific Research (Poland) [Grant No 3T09A 039 15]. E. G. B. thanks Mr Angelo M. Mitchell for financial support. A. T. thanks Mr John Boutaris and the Agricultural Bank of Greece (A.T.E.) for financial support.

References

1 A. K. Rappe and C. J. Casewit, *Molecular Mechanics across Chemistry*, University Science Books, Sausalito, CA, 1997.
2 A. Gavezzotti, *Acc. Chem. Res.*, 1994, **27**, 309.
3 M. C. Etter, *J. Phys. Chem.*, 1991, **95**, 4601; G. R. Desiraju, *Crystal Engineering, the Design of Organic Solids*, Elsevier, New York, 1989; S. Subramanian and M. J. Zaworotko, *Coord. Chem. Rev.*, 1994, **137**, 357; C. B. Aakeroy, *Acta Crystallogr.*, *Sect. B*, 1997, **53**, 569; J. C. MacDonald and G. M. Whitesides, *Chem. Rev.*, 1994, **94**, 2383.
4 B. F. Abrahams, B. F. Hoskins, D. M. Michail and R. Robson, *Nature* (*London*), 1994, **369**, 727; M. L. Mac Gillavray, S. Subramanian and M. J. Zaworotko, *J. Chem. Soc.*, *Chem. Commun.*, 1994, 1325; C. Janiak, *Angew. Chem.*, *Int. Ed. Engl.*, 1997, **36**, 1431; S. S.-Y. Chui, S. M.-F. Lo, J. P. H. Charmant, A. G. Orpen and I. D. Williams, *Science*, 1999, **283**, 1148; O. M. Yaghi, H. Li, C. Davis, D. Richardson and T. Groy, *Acc. Chem. Res.*, 1998, **31**, 474; D. Venkataraman, J. S. Moore and S. Lee, *Nature* (*London*), 1995, **374**, 792.
5 S. Katawata, S. Kitagawa, M. Kondo, I. Furuchi and M. Munakata, *Angew. Chem.*, *Int. Ed. Engl.*, 1994, **33**, 1759; O. M. Yaghi, H. Li and T. L. Groy, *J. Am. Chem. Soc.*, 1996, **118**, 9096; S. Katawata, S. Kitagawa, H. Kumagai, C. Kudo, H. Kamesaki, T. Ishiyama, R. Suzuki, M. Kondo and M. Katada, *Inorg. Chem.*, 1996, **35**, 4449; M. Munakata, L. P. Wu, M. Yamamoto, T. Kuroda-Sowa and M. Maekawa, *J. Am. Chem. Soc.*, 1996, **118**, 3117; A. D. Burrows, C. W. Chang, M. M. Chowdhry, J. E. McDrady, D. J. Williams and D. M. P. Mingos, *Chem. Soc. Rev.*, 1995, 329.
6 O. Asai, M. Kishita and M. Kubo, *J. Phys. Chem.*, 1959, **63**, 96.
7 M. P. Gupta and B. N. Saha, *Curr. Sci.*, 1978, **47**, 672.
8 A. Michaelides, D. Tsaousis, S. Skoulika, C. P. Raptopoulou and A. Terzis, *Acta Crystallogr.*, *Sect. B*, 1998, **54**, 657.
9 C. L. Schauer, E. Matwey, F. W. Fowler and J. W. Lauher, *J. Am. Chem. Soc.*, 1997, **119**, 10245.
10 M. S. Haddad and D. N. Hendrickson, *Inorg. Chem.*, 1978, **17**, 2622.
11 C. Boudias and D. Monceau, CaRIne Crystallography 3.1, Universite de Compiegne, France, 1998.
12 E. König, *Magnetic Properties of Coordination and Organometallic Transition Metal Compounds*, Springer-Verlag, Berlin, 1966.
13 G. M. Sheldrick, SHELXS 86: Structure Solving Program, University of Göttingen, 1986.
14 G. M. Sheldrick, SHELXL 93: Crystal Structure Refinement, University of Göttingen, 1993.
15 C. J. Carrell, H. L. Carrell, J. Erlebacher and J. P. Glusker, *J. Am. Chem. Soc.*, 1988, **110**, 8651.
16 G. R. Desiraju, *Angew. Chem.*, *Int. Ed. Engl.*, 1995, **34**, 2311.
17 J. Bernstein, R. E. Davis, L. Shimoni and N.-L. Chang, *Angew. Chem.*, *Int. Ed. Engl.*, 1995, **34**, 1555.
18 V. Tangoulis, S. Paschalidou, E. G. Bakalbassis, S. P. Perlepes, C. P. Raptopoulou and A. Terzis, *Chem. Commun.*, 1996, 1297; V. Tangoulis, C. P. Raptopoulou, S. Paschalidou, E. G. Bakalbassis, S. P. Perlepes and A. Terzis, *Angew. Chem.*, *Int. Ed. Engl.*, 1997, **36**, 1083; V. Tangoulis, C. P. Raptopoulou, A. Terzis, S. Paschalidou, S. P. Perlepes and E. G. Bakalbassis, *Inorg. Chem.*, 1997, **36**, 3996; C. P. Raptopoulou, S. Paschalidou, A. Pantazaki, A. Terzis, S. P. Perlepes, Th. Lialiaris, E. G. Bakalbassis, J. Mrozinski and D. A. Kyriakidis, *J. Inorg. Biochem.*, 1998, **71**, 15.
19 A. W. Addison, T. N. Rao, J. Reedijk, J. V. Rijn and G. C. Veerschoor, *J. Chem. Soc.*, *Dalton Trans.*, 1984, 1349.
20 E. G. Bakalbassis, E. Diamantopoulou, S. P. Perlepes, C. P. Raptopoulou, V. Tangoulis, A. Terzis and T. F. Zafiropoulos, *J. Chem. Soc.*, *Chem. Commun.*, 1995, 1347.
21 Y.-L. Chang, M.-A. West, F. W. Fowler and J. W. Fowler, *J. Am. Chem. Soc.*, 1993, **115**, 5991; J. W. Lauher, Y.-L. Chang and F. W. Fowler, *Mol. Cryst. Liq. Cryst.*, 1992, **211**, 99.
22 Y. Kuroda and M. Kubo, *J. Phys. Chem.*, 1960, **64**, 759.
23 G. B. Deacon and R. J. Phillips, *Coord. Chem Rev.*, 1980, **33**, 227.
24 R. L. Rardin, W. B. Tolman and S. J. Lippard, *New J. Chem.*, 1991, **15**, 417.
25 G. S. Rushbrooke and P. D. Wood, *J. Mol. Phys.*, 1958, **1**, 257.
26 C. A. Baker, H. E. Gilbert, J. Eve and G. S. Rushbrooke, *Phys. Lett. A*, 1967, **25**, 3.
27 C. P. Landee, D. M. Mudgett and B. M. Foxman, *Inorg. Chim. Acta*, 1991, **186**, 45.
28 P. J. Hay, J. C. Thibeault and R. Hoffmann, *J. Am. Chem. Soc.*, 1975, **97**, 4884.
29 M. S. Haddad, D. N. Hendrickson, J. P. Cannady, R. S. Drago and D. S. Bieksza, *J. Am. Chem. Soc.*, 1979, **101**, 898.
30 M. Julve and O. Kahn, *Inorg. Chem.*, 1984, **23**, 3808; A. Michalovicz, J.-J. Girerd and J. Goulon, *Inorg. Chem.*, 1979, **11**, 3004.
31 W. E. Hatfield, *Inorg. Chem.*, 1983, **22**, 833.
32 V. H. Crawford, H. W. Richardson, J. R. Wasson, D. J. Hodgson and W. E. Hatfield, *Inorg. Chem.*, 1976, **15**, 2107.